Electrical Power and Energy Systems 46 (2013) 79–88

Contents lists available at SciVerse ScienceDirect

Electrical Power and Energy Systems

journal homepage: www.elsevier.com/locate/ijepes

Controlling chaos and voltage collapse using an ANFIS-based composite controller-static var compensator in power systems

I.M. Ginarsa [a,b,*], A. Soeprijanto [b], M.H. Purnomo [b]

[a] Dept. of Electrical Engineering, Mataram University, Mataram, Indonesia
[b] Dept. of Electrical Engineering, ITS, Surabaya, Indonesia

ARTICLE INFO

Article history:
Received 21 June 2009
Received in revised form 31 August 2012
Accepted 9 October 2012
Available online 21 November 2012

Keywords:
Power systems
Chaos
Voltage collapse
ANFIS-based CC-SVC

ABSTRACT

Chaos and voltage collapse exist in power systems due to critical loading and disturbing of energy (DE). These phenomena cause instability in power system operation and must be avoided. In this paper, an ANFIS-based composite controller-static var compensator (CC-SVC) was proposed to control both chaotic oscillations and voltage collapse. The ANFIS-based CC-SVC was proposed because its computation was more efficient than Mamdani fuzzy logic controller. Adaptive network parameters were obtained through a training process. The controller parameters were automatically updated by off-line training. Both chaos and voltage collapse were able to control and suppress effectively by the proposed method. Furthermore, the load voltage was held to a set value by adjusting the supplied reactive power. When the reactive load was increased, the SVC susceptance and reactive power supplied by the SVC also increased. The proposed method was able to maintain the load voltage and to increase the loading margin.

1. Introduction

Chaos and voltage collapse are nonlinear phenomena that exist in power systems with critical (heavy) loading. Chiang et al. developed the voltage collapse model and described both the physical explanation and computational consideration of this model. Static and dynamic models were used to know the detailed type of voltage collapse, wherein the static model was used before a saddle-node bifurcation, while the dynamic model was employed after the bifurcation [1,2]. Meanwhile, the Lyapunov exponent which measured how rapidly the two nearby trajectories separate from one to another within the state space and broadband spectrum was used to confirm this observation [3]. Within the range of loading conditions, the sensitivity of chaotic behavior made power systems unpredictable after a finite time. In addition, the effectiveness of any control scheme was questionable within this range and should be reevaluated based on state vector information. Moreover, nonlinear phenomena, including bifurcation, chaos and voltage collapse occurred in power system models. The presence of various nonlinear phenomena was found to be a crucial factor in the inception of voltage collapse in this model [4,5]. The problem of control in the presence of these nonlinear phenomena is addressed here. The bifurcation control approach modified its bifurcation according to the system state equations and controlled chaos in power systems were done in [4–7]. The presence of chaotic oscillations in a power system causing the instability problem was studied by Yu et al. [8]. The existence of chaotic oscillations in power systems due to disturbing of energy (DE) at the rotor speed has been found in [9]. Furthermore, the modeling of chaotic behavior using recurrent neural networks in power systems was previously studied in [10]. Practical techniques for recognizing and classifying chaotic behavior were identified by Parker and Chua [11], while control and anti-control chaos were developed by Chen [12]. One scheme of chaos utility was used on electrical systems for smelting based on chaos control. Lei et al. demonstrated that chaotic steel-smelting ovens regulated their heating currents according to chaos control theory [13]. A control system using a neural-network controller was presumed to be able to stabilize the unstable focus points of 2-dimensional chaotic systems; although, Konishi and Kokame have stated that the control system did not require this presumption [14].

A fuzzy logic controller (FLC) has been successfully applied to control and stabilize chaotic systems, such as the Lorenz system [15] and the Chua circuit [16]. Various studies on controlling transient chaos have been carried out, such as those by Dhamala et al. and Dhamala and Lai attempted to control transient chaos in power systems using a data time-series [17,18]. Strategies for controlling chaos in process plants have been used on the discrete Henon map chaotic system [19]. A composite controller (CC) that has successfully controlled and suppressed chaos in power systems was reported in [4,5].

Static var compensator (SVC) placement is an attractive research topic in power system engineering. There have been many methods

* Corresponding author. Address: Dept. of Electrical Engineering, Faculty of Engineering, Mataram University, Jln. Majapahit No. 62, Mataram, NTB 83125, Indonesia. Tel.: +62 370 6608 703; fax: +62 370 636 755.
E-mail addresses: kadekgin@yahoo.com (I.M. Ginarsa), soeprijanto@its.ac.id (A. Soeprijanto), hery@its.ac.id (M.H. Purnomo).

0142-0615/$ - see front matter © 2012 Elsevier Ltd. All rights reserved.
http://dx.doi.org/10.1016/j.ijepes.2012.10.005

Nomenclature

ANFIS	adaptive neuro-fuzzy inference system
CC	composite controller
CVC	chaos to voltage collapse
DE	disturbing of energy
EP	equilibrium point
HI	high
MD	medium
MH	medium to high
NH	negative high
NL	negative low
LSE	least squares estimation
LM	low to medium
PL	positive low
PH	positive high
SM	small
SVC	static var compensator
VC	voltage collapse
TEM	trial and error method
ZE	zero
B_{svc}	SVC susceptance
c	membership function's center
E'_{q0}	voltage behind of direct reactance
Err	error percentage
k_l	linear gain
k_n	nonlinear gain
k_v	SVC gain
λ_1	additional reactive load, loading margin
Q_{svc}	reactive power supplied by the SVC
t_{svc}	SVC time constant
t_{v1}	time constant 1
t_{v2}	time constant 2
t_{ON}	SVC ON adjustment time
u, cs	control signal
V_{ref}	reference voltage
V	load voltage
V_{meas}	measurement voltage
V_{min}	minimum voltage
V_{ss}	steady-state voltage
x'_d	direct reactance
δ_m	rotor angle
$\Delta\omega$	rotor speed deviation
δ	voltage angle
ΔV	load voltage deviation
$\Delta V_{ss\text{-}svc}$	SVC voltage at steady state
$\Delta V_{r\text{-}svc}$	difference of reference and SVC voltage
$\Delta V_{t\text{-}svc}$	difference of terminal and SVC voltage
τ	membership function's width

applying the SVC placement optimally to maintain voltage stability, such as normal form analysis [20], multi-restart benders decomposition [21], reactive power spot price index (QSPI) [22] and genetic algorithms (GA) [23]. Meanwhile, a new SVC dynamic phasor simulator was proposed in order to substitute traditional electromagnetic transient program (EMTP) method [24]. Simulation results show that curves of a new method were very close to benchmark curves of EMTP. Furthermore, an SVC supplementary controller was applied to improve the damping of inter-area oscillations [25], SVC was used to suppress a Hopf bifurcation in power systems [26] and a phase compensator for SVC supplementary control was able to offset-time delay, to improve damping of inter-area oscillation and to enhance system stability [27].

Adaptive neuro-fuzzy inference systems (ANFIS) technology is a combination of neural networks and fuzzy inference systems. This technology has been applied to many engineering systems, including on the detection of inter-turn insulation and bearing wear faults in induction motors [28], as well as on supplementary controllers for damping low frequency oscillation in power systems [29] and automatic voltage regulators for generator systems [30].

In this paper, we focus on controlling chaotic oscillations and voltage collapse in power systems using an ANFIS-based CC-SVC. The ANFIS method was used in this research because its computational complexity was more effective than Mamdani fuzzy inference system. Furthermore, controller parameters were automatically updated by off-line training. This paper is organized as follows: the power systems used in this research are detailed in Section 2. Chaos and voltage collapse mechanisms in power systems are described in Section 3. Next, the ANFIS-based CC-SVC design is described in Section 4. The results and analysis are presented in Section 5. Finally, the conclusion is provided in the last section.

2. Power system model

A synchronous machine was modeled as a voltage $\left(E'_{q0}\right)$ behind a direct reactance (x'_d). The voltage magnitude was assumed as remaining constant at the pre-disturbance value. De Mello and Concordia, as well as Kundur, derived this model of a machine connected to an infinite bus [31]. Meanwhile, if saturation and the stator resistance were neglected, the system's condition was balanced with a static load. The machine was connected to the infinite bus and supplied the load. Then the armature current flowed from the machine to the load. This current caused electrical torque on the stator winding, and vice versa. The mechanical torque was produced by the flux through the rotor winding. Meanwhile, when the rotor speed was constant, the rotor speed followed the synchronous speed. When there was imbalanced energy, the rotor speed accelerated or decelerated, which can be expressed as follows:

$$\Delta\dot{\omega} = \frac{1}{M}(T_m - T_e - D\Delta\omega) \tag{1}$$

where T_m, T_e, $\Delta\omega$, D and M are the mechanical torque, electrical torque, rotor speed deviation, damping constant and inertia constant, respectively. This system model was developed from the work of Chiang et al. [1], as shown in Fig. 1. This model represents the system as a synchronous machine that supplies power to a local dynamic load with a shunt capacitor (Bus 2) connected by a weak tie line to an external system (Bus 3). The equations of infinite bus were described as follows:

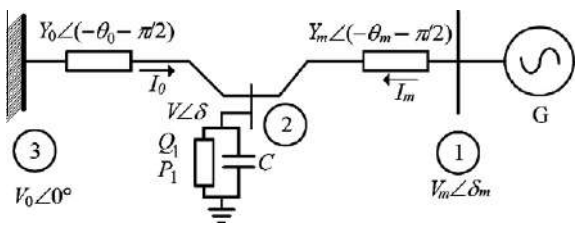

Fig. 1. Three-bus power systems.

$$V_0' = \frac{V_0}{\left[1 + C^2 Y_0^{-2} - 2CY_0^{-1}\cos(\theta_0)\right]^{0.5}} \quad (2)$$

$$Y_0' = Y_0\left[1 + C^2 Y_0^{-2} - 2CY_0^{-1}\cos(\theta_0)\right]^{0.5} \quad (3)$$

$$\theta_0' = \theta_0 + \arctan\left[\frac{CY_0^{-1}\sin(\theta_0)}{1 - CY_0^{-1}\cos(\theta_0)}\right] \quad (4)$$

By using the variables and parameters in Table 1, the V_0', Y_0', θ_0' were obtained as follows: $V_0' = 2.5$ pu, $Y_0' = 8.0$ pu, $\theta_0' = -0.209$ rad. Thus, power system equations are defined as follows:

$$\dot{\delta_m} = \Delta\omega \quad (5)$$

$$\Delta\dot{\omega} = \frac{1}{M}[-D\Delta\omega + P_m + V_m^2 Y_m \sin(\theta_m) + V_m V Y_m \sin(\delta - \delta_m - \theta_m)] \quad (6)$$

$$\dot{\delta} = \frac{1}{K_{q\omega}}[-K_{qv}V - K_{qv2}V^2 + Q - Q_0 - Q_1] \quad (7)$$

$$\dot{V} = \frac{1}{TK_{q\omega}K_{pv}}[K_{p\omega}K_{qv2}V^2 + (K_{p\omega}K_{qv} - K_{q\omega}K_{pv})V + K_{p\omega}(Q_0 + Q_1 - Q) - K_{q\omega}(P_0 + P_1 - P) + u(\Delta\omega)] \quad (8)$$

where the parameters $K_{p\omega}$, K_{pv}, $K_{q\omega}$, K_{qv}, K_{qv2} and T are the active load constant due to frequency deviation, active load constant due to voltage deviation, reactive load constant due to frequency deviation, reactive load constant due to voltage deviation, reactive load constant due to voltage square deviation and time constant, respectively. The variables δ_m, $\Delta\omega$, δ and V are the power angle, rotor speed deviation, angle and magnitude of the voltage. The variables P and Q were computed using Eqs. (9) and (10), respectively. The parameters P_1, Q_1 and D are the real load, reactive load and damping constant. In this case, the parameter $u(\Delta\omega)$ was implemented as a control signal of the power systems.

$$P = -V_0' V Y_0' \sin(\delta + \theta_0') - V_m V Y_m \sin(\delta - \delta_m + \theta_m) + [Y_0' \sin(\theta_0') + Y_m \sin(\theta_m)]V^2 \quad (9)$$

$$Q = V_0' V Y_0' \cos(\delta + \theta_0') + V_m V Y_m \cos(\delta - \delta_m + \theta_m) - [Y_0' \cos(\theta_0') + Y_m \cos(\theta_m)]V^2 \quad (10)$$

Eqs. (5)–(8) were simplified into a single formula as follow

$$\dot{x} = f(x, \lambda) \quad (11)$$

where $x \in \mathbb{R}^n$, $\lambda \in \mathbb{R}^p$, x and λ are the state variable and parameter space, respectively. The state variable is $x = [\delta_m\ \Delta\omega\ \delta\ V]^T$, wherein the superscript T denotes the transpose of the associate vector. The parameter space was interpreted as a loading margin (λ_1):

$$\lambda_1 = \lambda_{max} - \lambda_0 \quad (12)$$

where λ_{max} and λ_0 are the critical and initial reactive load, respectively.

3. Chaos and voltage collapse

3.1. Chaos phenomena in power systems

Chaos refers to one type of complex dynamical behavior that possesses some very special features, such as being extremely sensitive to tiny variations of parameters and initial conditions and having bounded trajectories in the phase-plane, but with a positive

Table 1
Power system parameter values.

Y_0	Y_m	V_0	V_m	θ_0	θ_m	P_m	M	D
20.0	5.0	1.0	1.0	−5.0	−5.0	1.0	0.3	0.05
$K_{p\omega}$	K_{pv}	$K_{q\omega}$	K_{qv}	K_{qv2}	C	P_0	Q_0	T
0.4	0.3	−0.03	−2.8	2.1	12.0	0.6	1.3	8.5

All parameter values are in pu except for angles, which are in degs.

Table 2
Chaos and voltage collapse due to initial condition and parameter variation.

DE (rad s^{-1})	Reactive load $\times j$ (pu)	Quality behavior	Label	Time (s)	Phase-plane trajectory
0.5		EP	–	1,025	–
1.274398231696		EP	A	2,070	–
1.274398231697		chaos	B	∞	–
1.670052980343		chaos	C	∞	Fig. 2
1.670052980344		EP	D	1,768	Fig. 3
1.670052980346		EP	E	2,350	–
1.670052980347		chaos	F	∞	–
1.670052980348	10.89	EP	G	2,436	–
1.670053018411		EP	H	800	–
1.670053018412		VC	I	1.6774	Fig. 4
1.670053018413		VC	J	1.6375	
1.670053018414		VC	K	1.6181	
1.670053018419		VC	L	1.5745	
1.670053018442		VC	M	1.5186	
	10.87	EP	N	1,180	–
	10.8976811	EP	O	1,210	–
1.2	10.89768110001	CVC	P	4,500	–
	10.89768110002	EP	Q	4,300	–
	10.899	CVC	R	442.315	Fig. 5

EP: Equilibrium point
VC: Voltage collapse
CVC: Chaos to voltage collapse

maximum Lyapunov exponent and/or a fractional topological dimension. The definition of chaos, its properties [32], and its applications in engineering systems have been described in [34,35]. The appearance of chaos can be described by the existing route to chaotic behavior in power systems caused by rotor speed deviation. The rotor speed deviation in power systems was affected by the DE. Kinetic energy disturbances were exclusively related to the rotor speed deviation. For the sake of simplicity, the rotor speed deviation in Table 2 was labeled from A to M. When DE value < A, power systems were able to converge to a stable equilibrium point. When the DE was increased, convergence became more difficult than before. When the DE value at B, power systems took longer to chaotic oscillation (chaos) as shown in Fig. 2. In the B, C and F intervals, the system was controlled by chaos. Next, when the DE value was increased again from intervals D to E and G to H, the system was in equilibrium point as shown in Fig. 3. Furthermore, when the DE value > I, the system went to voltage collapse (VC).

3.2. Voltage collapse mechanism in power systems

Voltage collapse is a problem in dynamical voltage stability analysis that occurs when power systems are under critical loading and/or deficits of reactive load. Owing to ever-increasing load demands, there is tremendous interest in operating power systems very near the edge of their stability boundaries. A disturbance and/or temporal overload caused a shift in a system parameter, such that a boundary crisis occurred, after which the system exhibited transient chaos, leading to voltage collapse (VC). In Table 2, the VC mechanism was divided into two mechanisms: from chaos to voltage collapse (CVC) due to reactive load (parameter) increased and direct VC due to DE (initial condition) increased. The VC and CVC are shown in Figs. 4 and 5, respectively.

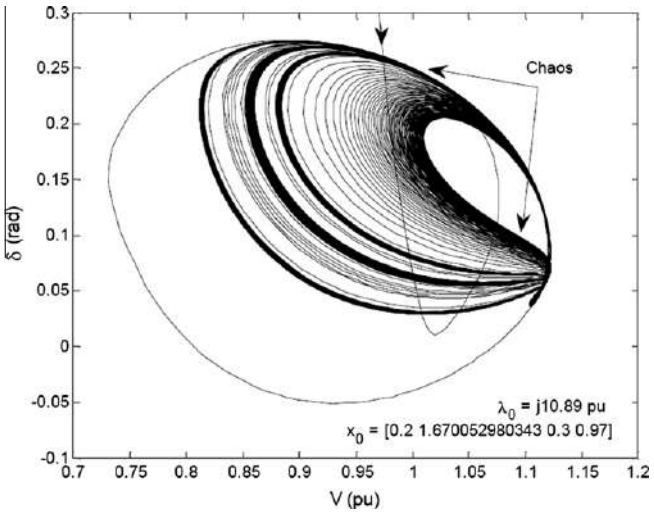

Fig. 2. Chaos occurred in the $\delta - V$ trajectories.

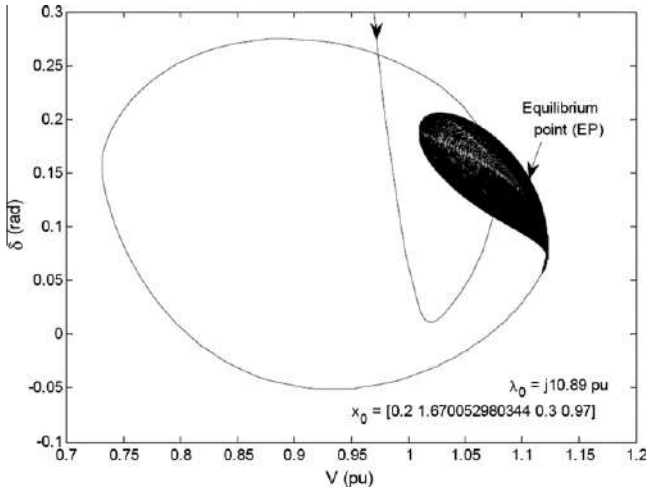

Fig. 3. Equilibrium point (EP) was achieved at time of 1768 s.

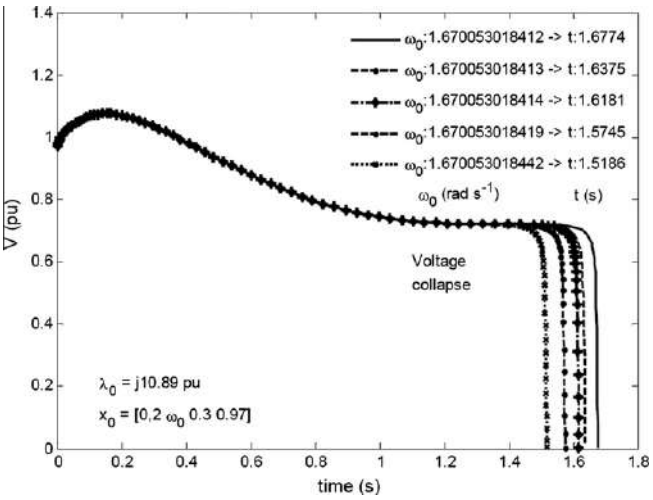

Fig. 4. Temporal response of the voltage collapse (VC).

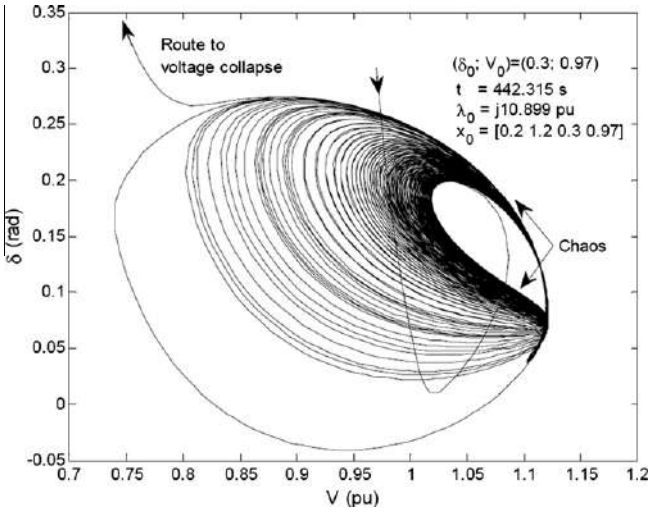

Fig. 5. Chaos to voltage collapse (CVC) occurred at 442.315 s.

4. ANFIS-based CC-SVC design

4.1. Composite controller-SVC conventional

4.1.1. Composite controller (CC)

Two type of control law, consist of: linear controller and cubic controller were combined to produce composite controller. The function of linear controller was to improve both static and dynamic stability margins. Meanwhile, the function of cubic controller was to avoid chaos, voltage collapse and to improve stability degree [4]. The formulation of linear and cubic controller with measurement of u and $\Delta\omega$, can be expressed as follows:

$$u = k_l \Delta\omega + k_n (\Delta\omega)^3 \tag{13}$$

where the variable $\Delta\omega$ is rotor speed deviation, parameters u, k_l and k_n are the control signal, linear gain and nonlinear gain, respectively. The parameters k_l and k_n were adjusted at the values of 0.8 and 0.8, respectively. Block diagram of the CC is shown in Fig. 6.

4.1.2. SVC controller

Let us start with SVC that was applied at bus k, and the reactive power was injected to bus k

$$Q_k = V_k^2 B_{svc} \tag{14}$$

where $B_{svc} = B_c - B_l$, B_{svc}, B_c and B_l, are the SVC, capacitive and inductive susceptances, respectively. Dynamic formulas of SVC is written as follow [33]:

$$\Delta\dot{B}_{svc} = \frac{1}{t_{svc}}\left[\left(1 - \frac{t_{v1}}{t_{v2}}\right)\Delta V_{r-svc} - \Delta B_{svc} - k_v \frac{t_{v1}}{t_{v2}}\Delta V_{t-svc}\right] + k_v \frac{t_{v1}}{t_{v2} t_{svc}}(\Delta V_{ss-svc} + V_{ref}) \tag{15}$$

where t_{svc}, t_{v1}, t_{v2}, k_v, ΔV_{ss-svc}, ΔV_{r-svc}, ΔV_{t-svc} and V_{ref} are the SVC time constant, time constant 1, time constant 2, SVC gain, SVC voltage at steady state, difference of reference and SVC voltage, difference of terminal and SVC voltage, and reference voltage, respectively. And parameter values of SVC for the t_{svc}, t_{v1}, t_{v2} and k_v were 70.0, 3.0729 117.96, 400.0 and 30.0, respectively. Block diagram of the SVC is shown in Fig. 7. Meanwhile, block diagram of proposed method applied to power systems is shown in Fig. 8.

4.2. Design processes of ANFIS-based CC-SVC

A step-by-step method of ANFIS-based CC-SVC design is presented as follows:

1. Selection of input variables: In this step, the state variables provided as input signals to the controller were chosen.
   (a) The rotor speed deviation ($\Delta\omega$) and its derivative ($\Delta\dot{\omega}$) were the input signals for the ANFIS-based CC.
   (b) The voltage angle (δ) and measurement voltage (V_{meas}) were the input signals for the ANFIS-based SVC.
2. Selection of linguistic variables: Five linguistic variables were used to describe each of the input variables.
   (a) Negative high (NH), negative low (NL), zero (ZE), positive low (PL) and positive high (PH) for the CC.
   (b) Small (SM), low to medium (LM), medium (MD), medium to high (MH) and high (HI) for the SVC.

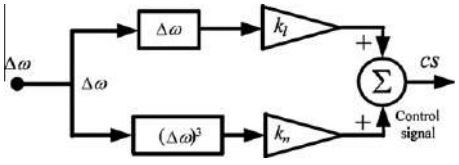

Fig. 6. Composite controller block diagram.

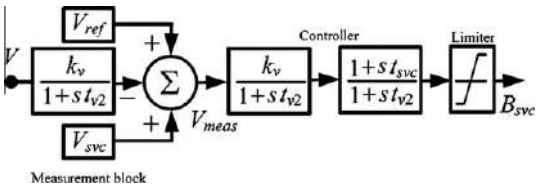

Fig. 7. SVC controller block diagram.

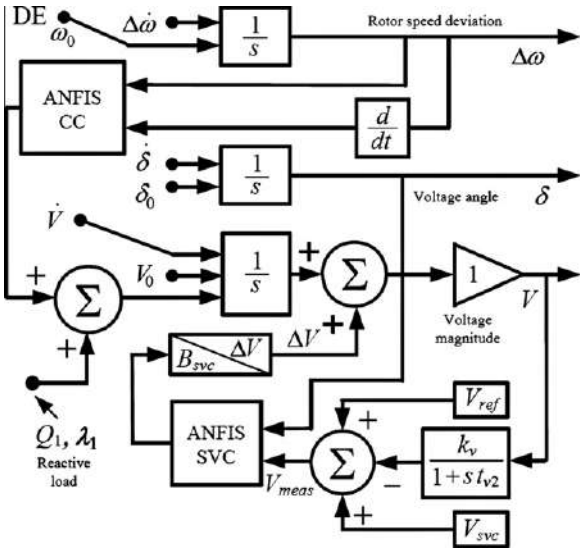

Fig. 8. ANFIS-based CC-SVC block diagram.

3. Selection of membership functions: Gaussian membership functions were used to define the degree of membership of input variables. A Gaussian membership function was specified by two parameters (c, τ), where c and τ represent the membership function's center and width (spread), respectively. These parameters were obtained automatically through learning processes by a hybrid algorithm [34,35].
4. Selection of fuzzy model: A first-order fuzzy model Sugeno (T-S) was chosen in this design because of its computational efficiency.
5. Preparation of training data pairs: There were two sets of data training pairs:
   (a) The rotor speed deviation, its derivative and a control signal (cs) as the two inputs and output of the ANFIS-based CC, respectively.
   (b) The voltage angle (δ), measurement voltage (V_{meas}) and SVC susceptance (B_{svc}) as the two inputs and output for the ANFIS-based SVC, respectively.
6. Optimization of unknown parameters: The unknown parameters of the Gaussian membership function, such as center and spread, and the linear output of each rule of the first-order Sugeno fuzzy model were optimized by using a matrix of training data pairs. All initial values for the center and the spread of each input membership function were assumed as zero for each rule. Furthermore, the input and output parameters were optimized using the back-propagation algorithm and least squares estimation (LSE) method, respectively.

4.3. Training process for ANFIS-based CC-SVC parameters

The training processes were performed using off-line methods with 6000 data points. The training of data pairs were prepared by simulating power systems with a conventional CC-SVC. By this training, the values for the number of nodes, number of linear parameters, number of nonlinear parameters and number of fuzzy rules were obtained at 75, 75, 20 and 25, respectively. Each input parameter was represented by five Gaussian membership functions. The input–output surfaces of the ANFIS-based CC-SVC are described in Figs. 9 and 10, respectively.

Fig. 9 shows the relationship of two inputs ($\Delta\omega$; $\Delta\dot{\omega}$) and an output cs with two maximum values and two minimum values. The first maximum value was achieved at 0.12 when the input for the rotor speed deviation and its derivative were at the values

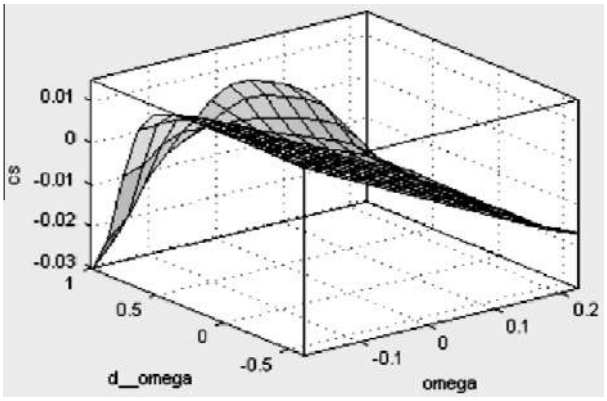

Fig. 9. Input–output control surface of ANFIS-based CC.

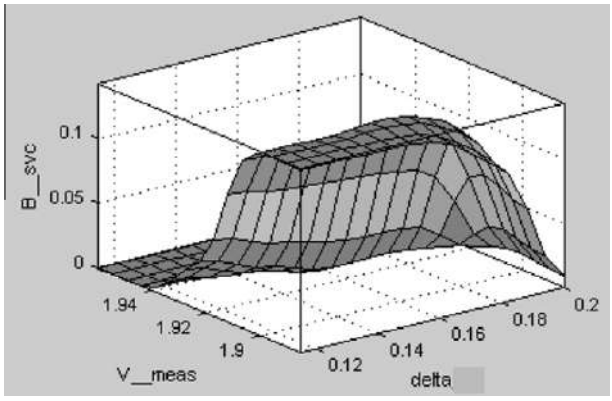

Fig. 10. Input–output control surface of ANFIS-based SVC.

of −0.186 rad s^{-1} and −0.512 rad s^{-2}, respectively. The control signal in this case did not have any dimension unit. Meanwhile, second hill was achieved at the value of 0.0095 when the input for rotor speed deviation and its derivative were at the values of 0.045 rad s^{-1} and 1.0 rad s^{-2}, respectively. On the contrary, the first minimum value was achieved at −0.03 when the input for the rotor speed deviation and its derivative were at the values of −0.085 rad s^{-1} and 1.0 rad s^{-2}, respectively. And the second minimum value was achieved at −0.023 when the input for rotor speed deviation and its derivative were at the values of 0.2 rad s^{-1} and −0.53 rad s^{-2}, respectively.

Fig. 10 shows the nonlinear of voltage angle (δ) as an input 1; measurement voltage (V_{meas}) as an input 2 and SVC susceptance (B_{svc}) as an output. Firstly, the control surface of the SVC susceptance is shown from voltage angle side. The SVC susceptance increased from 0.015 to 0.023 pu when the voltage angle was from 0.2 to 0.193 rad. Furthermore, the SVC susceptance sharply increased from 0.0231 to 0.0894 pu when the voltage angle was from 0.1821 to 0.181 rad. Meanwhile, the SVC susceptance moderately increased from 0.0895 to 0.141 pu when the voltage angle was from 0.1812 to 0.124 rad. Secondly, the control surface is shown from measurement voltage side. The SVC susceptance stayed at 0.0 pu when the measurement voltage was from 1.96 to 1.945 pu and the voltage angle was at the value of 0.11 rad. The SVC susceptance increased from 0.0 to 0.024 pu when the measurement voltage was decreased from 1.944 to 1.928 pu. Furthermore, the SVC susceptance sharply increased from 0.024 to 0.140 pu when the measurement voltage was decreased from 1.944 to 1.921 pu. Meanwhile, the SVC susceptance moderately increased and stayed at the value of 0.141 pu when the measurement voltage at the values was from 1.920 to 1.86 pu.

5. Results and analysis

Performance of the proposed method was examined using Matlab/Simulink V.7.6.0 324 on an Intel Core 2 Duo E6650 233 GHz PC computer. The simulations were done as follows:

1. The DE and initial reactive load (λ_0) were added to power systems without any control device, and the responses of the systems were observed. The simulation results are presented in Figs. 2–5 and Table 2.
2. Next, a slightly reactive load was added to power systems with a conventional composite controller (conventional CC). The results are presented in Table 3.
3. Furthermore, power systems were equipped by the proposed method (ANFIS-based CC-SVC) and two scenarios were taken and illustrated as follows:
   (a) Scenario 1: The DE was added to the rotor speed at the generator bus in 4 stages: 1.27, 1.3, 1.325 and 1.35 rad s^{-1}. The results are presented in Table 4.
   (b) Scenario 2: The reactive load was added to the load bus with 0.04 pu per step. Reference voltage was taken at the values of 0.98, 0.985, 0.99 and 0.995 pu. The simulation results are listed in Table 5.

5.1. Power systems without control device

Power systems without any control schemes were very vulnerable to disturbances during operation. The disturbances used were DE and reactive load, as the initial condition and parameter, respectively. The power system behavior changed qualitatively when both the initial condition and the parameter was changed.

Table 3
Performance of conventional CC and proposed method at λ_0:*j*11.27 pu.

Conventional CC				Proposed method			
$\lambda_1 \times j$ (pu)	δ (rad)	Load V_{min} (pu)	Voltage V (pu)	$\lambda_1 \times j$	δ (rad) (pu)	Load V_{min} (pu)	Voltage V (pu)
0.0	0.1359	0.9224	0.9770	0.0	0.1352	0.9334	0.9800
0.01	0.1365	0.8955	0.9712	0.02	0.1338	0.9325	0.9800
0.011	0.1365	0.8899	0.9706	0.04	0.1324	0.9300	0.9801
0.012	0.1366	0.8818	0.9699	0.06	0.1310	0.9287	0.9799
0.0125	0.1366	0.8729	0.9696	0.08	0.1296	0.9274	0.9800
0.01275	0.1367	0.8616	0.9695	0.10	0.1282	0.9265	0.9800
0.012772	0.1367	0.8571	0.9695	0.12	0.1267	0.9236	0.9799
0.0127721	0.1367	0.8570	0.9695	0.14	0.1253	0.9222	0.9803
0.0127726052101	0.1367	0.8567	0.9695	0.16	0.1239	0.9163	0.9807
–	–	–	–	0.18	0.1189	0.8943	0.9810
–	–	–	–	0.20	0.1173	0.8785	0.9814

Table 4
Performance of the proposed method for the DE variation.

DE (rad s^{-1})	V_{ref} = 0.98 pu		V_{ref} = 0.985 pu	
	t_{ON}(s)	B_{svc}; Q_{svc}; V (pu)	t_{ON} (s)	B_{svc}; Q_{svc}; V(pu)
1.2744	1.9247		1.8914	
1.30	1.9797	B_{svc}: $-j0.4063$	1.9609	B_{svc}: $-j0.3943$
1.325	2.0478	Q_{svc}: $-j0.4013$	2.665	Q_{svc}: $-j0.3825$
1.35	3.3204	V:0.98	2.83	V:0.985
	V_{ref} = 0.99 pu		V_{ref} = 0.995 pu	
1.2744	1.8643		1.8185	
1.30	1.9364	B_{svc}: $-j0.3813$	1.8930	B_{svc}: $-j0.3677$
1.325	2.0226	Q_{svc}: $-j0.3737$	2.0036	Q_{svc}: $-j0.3640$
1.35	2.8019	V:0.99	2.737	V:0.995

Both the DE and reactive load were increased step by step, and the responses in the phase-plane trajectory were observed. Four types of qualitative behavior have been observed in power system operation such as: Chaos (Fig. 2), equilibrium point (EP, Fig. 3), voltage collapse (VC, Fig. 4) and chaos to voltage collapse (CVC, Fig. 5). Furthermore, the qualitative behavior of power systems are described in Table 2.

5.2. Power systems with conventional CC

Power systems equipped by a conventional CC was able to control chaos and voltage collapse, but the load voltage remains uncontrolled and fluctuated, according to reactive load changed. The power system may be operated in an over-voltage/under-voltage mode when the reactive load was taken at light/heavy values. When power systems were under critical (heavy) load and the reactive load was slightly increased, the load voltage declined rapidly to voltage collapse.

Power system responses by changing reactive loads are depicted in Table 3. Three variables were observed in this simulation such as: The voltage angle, minimum voltage (V_{min}) and steady-state voltage (V). The minimum voltages were obtained 0.9224, 0.8955 and 0.8567 pu for the reactive load at its initial value, j0.01 and j0.0127726 pu, respectively. And the steady-state voltages were obtained at the values of 0.9770, 0.9712 and 0.9695 pu for the reactive load at its initial value, j0.01 and j0.0127726 pu, respectively. The load voltage variation was strongly depends on the reactive load. Meanwhile, the voltage angle slightly increased from 0.1359 to 0.1367 rad when the reactive load was increased from initial value to j0.01277 pu. Furthermore, systems with a conventional CC was able to control the rotor speed deviation. Unfortunately, this controller was not able to maintain the load voltage because its controller did not have reactive power control device.

The load voltage dynamics of the CC are described in Fig. 11. The voltage stability can be observed in the minimum voltage, which rapidly decreased when the reactive load was slightly increased. As illustrated, the minimum voltage at the value of 0.9224 pu when the reactive load was at the initial value, while its value immediately decreased to 0.8567 pu when the reactive load was slightly increased. When the reactive load were increased again, then voltage collapse occurred due to lack of reactive power in the networks.

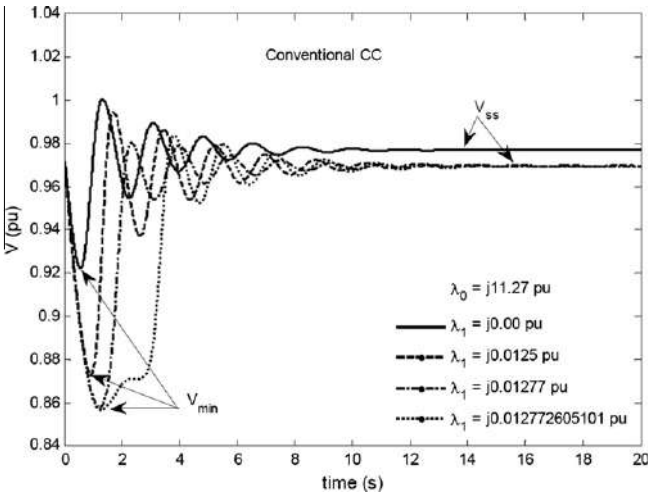

Fig. 11. Load voltage responses of conventional CC with various reactive loads.

Table 5
Performance of the proposed method for reactive load variation.

λ_0:j11.27 pu V_{ref}: 0.98 pu					V_{ref} = 0.985 pu			
$\lambda_1 \times j$ (pu)	$B_{svc} \times j$ (pu)	$Q_{svc} \times j$ (pu)	V (pu)	Err (%)	$B_{svc} \times j$ (pu)	$Q_{svc} \times j$ (pu)	V (pu)	Err (%)
0.0	0.0084	0.0081	0.9800	0.0	0.0181	0.0176	0.9850	0.0
0.04	0.0510	0.0490	0.9801	0.01	0.0628	0.0609	0.9850	0.0
0.08	0.0958	0.0920	0.9800	0.0	0.1077	0.1045	0.9850	0.0
0.12	0.1410	0.1354	0.9799	0.01	0.1529	0.1483	0.9850	0.0
0.16	0.1906	0.1833	0.9807	0.07	0.1983	0.1924	0.9850	0.0
0.20	0.2377	0.2289	0.9814	0.14	0.2441	0.2368	0.9850	0.0
0.24	–	–	–	–	0.2901	0.2815	0.9851	0.01
0.28	–	–	–	–	0.3367	0.3267	0.9851	0.01
λ_0:j11.37 pu V_{ref} = 0.99 pu					V_{ref} = 0.995 pu			
0.0	0.0285	0.0280	0.9900	0.0	0.0398	0.0394	0.9950	0.0
0.04	0.0730	0.0716	0.9901	0.01	0.0841	0.0833	0.9951	0.01
0.08	0.1178	0.1154	0.9900	0.0	0.1287	0.1274	0.9950	0.0
0.12	0.1628	0.1596	0.9900	0.01	0.1735	0.1718	0.9950	0.0
0.16	0.2081	0.2040	0.9900	0.07	0.2187	0.2165	0.9951	0.01
0.20	0.2537	0.2486	0.9902	0.02	0.2641	0.2615	0.9949	0.01
0.24	0.2901	0.2936	0.9900	0.00	0.3098	0.3067	0.9949	0.01
0.28	0.3457	0.3388	0.9903	0.03	0.3557	0.3522	0.9952	0.02
0.32	0.3921	0.3842	0.9900	0.01	0.4020	0.3980	0.9953	0.03
0.36	0.4389	0.4301	0.9900	0.00	0.4487	0.4443	0.9951	0.01
0.37	0.4507	0.4418	0.9990	0.14	0.4603	0.4557	0.9950	0.0
0.38	–	–	–	–	0.4956	0.4907	0.9950	0.0
0.42	–	–	–	–	0.5192	0.5141	0.9951	0.01
0.46	–	–	–	–	0.5674	0.5622	0.9954	0.04

5.3. Power systems with the proposed method

The proposed method is used to control both chaos and voltage collapse in power systems. Chaos and voltage collapse control are provided by the ANFIS-based CC- and SVC, respectively. Voltage regulation is the main function of the SVC device, through control of SVC susceptance.

5.3.1. Scenario 1

In this scenario, the proposed method was tested using the DE at the rotor speed deviation. The performance of the proposed method when the DE at the values of 1.27439, 1.3, 1.325 and 1.35 rad s^{-1} forced to the power systems are listed in Table 4. In this simulation the reference voltage was taken to be 0.98 pu, the SVC ON adjustment time (t_{ON}) was taken the at time of 1.9247, 1.9797, 2.0478 and 3.3204 s for DE values of 1.274398, 1.3, 1.325 and 1.35 rad s^{-1}, respectively. When the DE was increased, then t_{ON} also increased. On the contrary, the SVC ON adjustment time decreased when the reference voltage was increased. The shortest of the t_{ON} was at time of 1.8185 s, for the DE of 1.274398 rad s^{-1} and a reference voltage of 0.995 pu. The SVC susceptance and the reactive power absorbed by the SVC were $-j0.4063$ and $j0.4013$ pu, respectively, for a reference voltage of 0.98 pu. The SVC susceptance and the reactive power absorbed by the SVC decreased when the reference voltage was increased. Stress on the power systems also increased when the DE was increased. It was more difficult to rapidly reduced this disturbance. Voltage collapse occurred when the load voltage decreased too early. In order to avoid the voltage collapse caused by the reduction of the load voltage too early, the proper t_{ON} must be realized.

Fig. 12 shows that the equilibrium point was achieved by the phase plane (V;δ) trajectories at coordinate (0.98; 0.16) when the DE and t_{ON} at the values of 1.27439 rad s^{-1} and 1.9247 s, respectively. Meanwhile, Fig. 13 demonstrates the comparison of conventional CC and the proposed method when the DE was forced at generator bus. It is shown that the load voltage uncontrolled and stayed at the high value (1.086 pu) when power systems equipped by conventional CC. On the other hand, the load voltage was able to control at the value of 0.98 pu when the power systems equipped by the proposed method.

5.3.2. Scenario 2

Performance of the proposed method was evaluated by adding a reactive load at the load bus and observing the reaction of the SVC susceptance (B_{svc}), reactive power supplied by the SVC (Q_{svc}), and the load voltage (V) at different reference voltage (V_{ref}) in this sce-

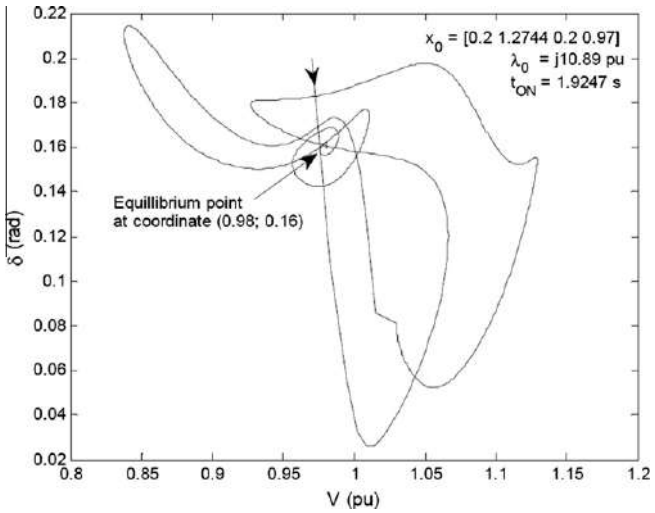

Fig. 12. Equilibrium point was achieved at coordinate (0.98; 0.16).

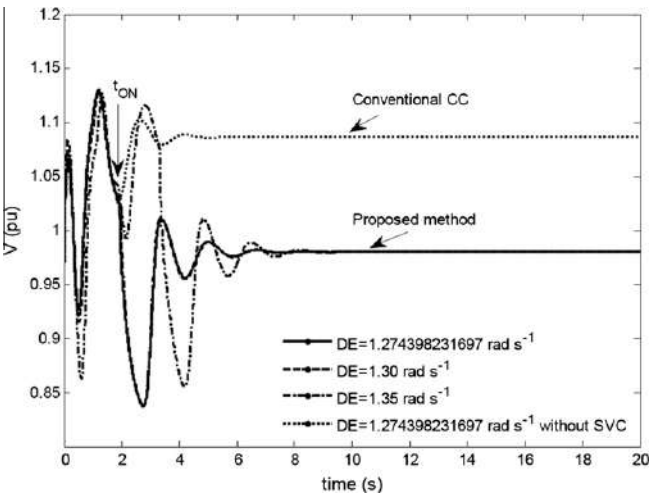

Fig. 13. Comparison of load voltage responses when DE was forced to power systems.

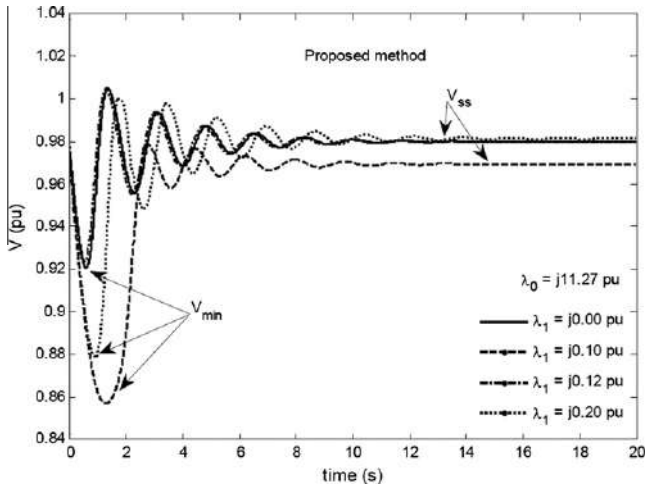

Fig. 14. Load voltage responses of the proposed method with various reactive loads.

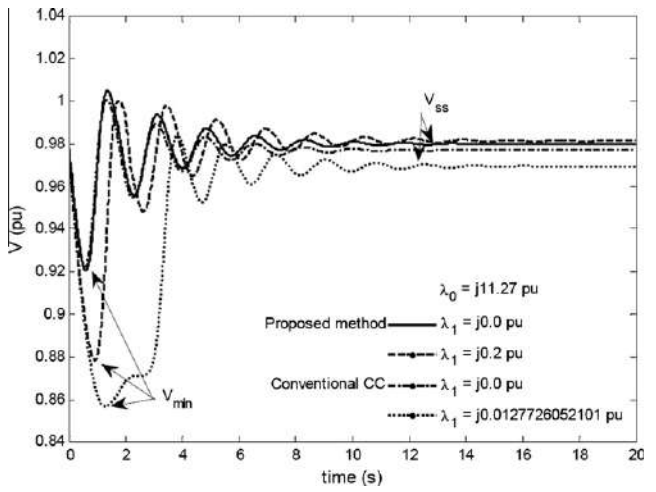

Fig. 15. Comparison of the V responses when power systems were forced by minimum and maximum reactive loads.

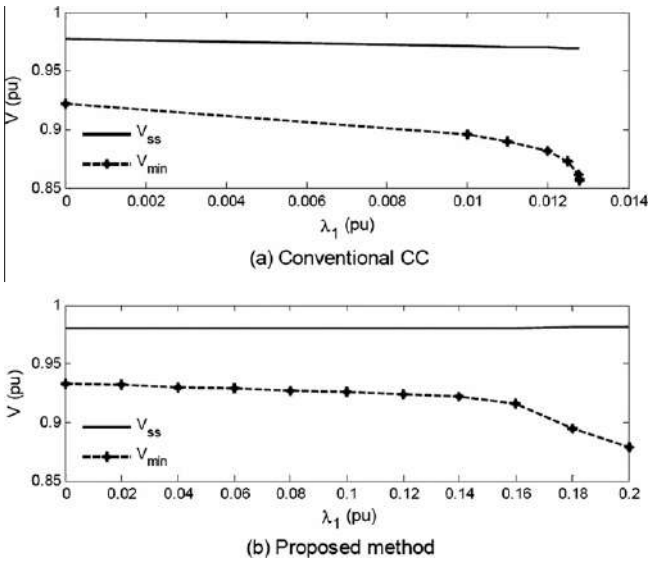

Fig. 16. Comparison of V_{ss} and V_{min} for the proposed method and conventional CC.

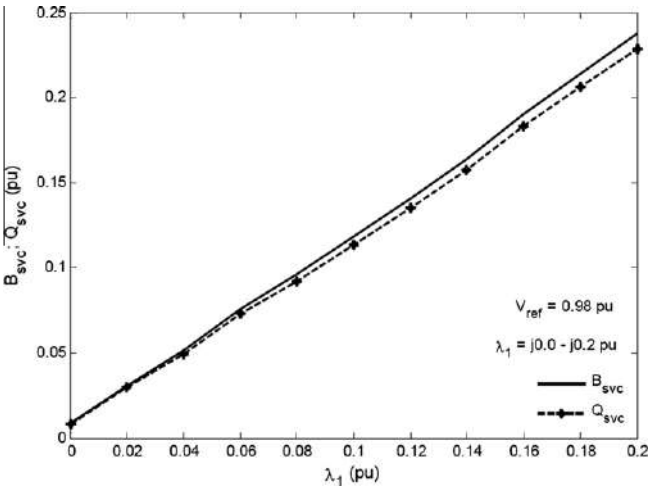

Fig. 17. SVC susceptance and reactive power supplied by the SVC against λ_1.

Table 6
Loading margin of the proposed method for reference voltage variation.

V_{ref} (pu)	$\lambda_0 \times j$ (pu)	$\lambda_{max} \times j$ (pu)	$\lambda_1 \times j$ (pu)
0.98	11.27	11.47	0.2
0.985	11.27	11.55	0.28
0.99	11.37	11.74	0.37
0.995	11.37	11.83	0.46

nario. The simulation results of the proposed method are in Figs. 14–17 and Tables 5 and 6.

Fig. 14 shows the performance of the proposed method when the load bus was forced by reactive load. The reactive load was varied from initial value to j0.2 pu and the load voltage was able to control at the value of 0.98 pu. Furthermore, the load voltage dynamics were significantly improved by using the proposed method. Meanwhile, the minimum voltages varied depending on the reactive load. As discussed before, when the reactive load was increased made the minimum voltage decreased. When the reactive load was at its initial value, the resulting minimum voltage was 0.9334 pu. Furthermore, when the reactive load increased to j0.2 pu, then the minimum voltage decreased to 0.8785 pu.

Fig. 15 shows the load voltage responses of the proposed method at $\lambda_1 = j0.0$; j0.2 pu and conventional CC at $\lambda_1 = j0.0$; j0.012772 pu. From Fig. 15, we can see that the proposed method was better than conventional CC. Power systems equipped by the proposed method was able to handle the λ_1 at the value of j0.2 pu. Meanwhile, the ability of power systems using conventional CC was limited at the λ_1 of j0.012772 pu. In addition, the V_{min} of the proposed method was achieved at the value of 0.8785 pu for the $\lambda_1 = j0.2$ pu; the V_{min} of the conventional CC was at the value of 0.8567 pu for the $\lambda_1 = j0.012772$ pu. Finally, the V of the proposed method was at the value of 0.9814 pu for the $\lambda_1 = j0.2$ pu; the V of conventional CC at 0.9695 pu for the $\lambda_1 = j0.012772$ pu.

Fig. 16 demonstrates the performance of the proposed method (ANFIS-based CC-SVC) and the conventional CC. The performances are assessed by the graph of additional reactive load vis steady-state and minimum voltage. Fig. 16a shows that the steady-state and minimum voltage sharply decreased when the reactive load was slightly increased. Meanwhile, when the proposed method was applied, the steady-state voltage was held at around of 0.98 pu (Fig. 16b). And the minimum voltage regularly decreased until the reactive load was around j0.16 pu. Furthermore, the minimum voltage sharply decreased when the reactive load was around j0.2 pu (Fig. 16b).

Fig. 17 illustrates the SVC susceptance and the reactive power supplied by the SVC device. Both the SVC susceptance and reactive power supplied by the SVC increased when the reactive load was increased at the load bus. The SVC susceptance needs to increase to keep the load voltage at the set value when the reactive load in a power system varies. The reactive power supplied by the SVC needs to maintain reactive power balance in the power system to prevent voltage collapse under critical (heavy) loading. The error percentage of the reference voltage and load voltage were used to validate the proposed method. The error percentage was obtained from the difference between the reference voltage and load voltage: where the reference voltages were taken at the fixed values of 0.98, 0.985, 0.99 and 0.995 pu and the load voltages were observed on the load bus. From Table 5, it can be seen that the load voltage error was from 0.0% to 0.14%. This error was sufficiently small. The SVC susceptance ranged from j0.0084 to j0.2377 pu when the reference voltage was set to 0.98 pu. At this setting, the additional reactive load (loading margin, λ_1) that could be handled was j0.2 pu, with a load voltage at the value of 0.9814 pu. As described in Table 5, the SVC susceptance and load voltage increased when the reference voltage was increased. The SVC susceptance ranged from j0.0398 to j0.5674 pu at a reference voltage of 0.995 pu. At this setting, the loading margin was achieved at the value of j0.46 pu at a load voltage of 0.9954 pu.

The reactive power supplied by the SVC increased from j0.0084 to j0.2289 pu as the additional reactive load was increased from j0.0 to j0.2 pu at a reference voltage of 0.98 pu. The maximum reactive power supplied by the SVC was j0.5622 pu, at the loading margin of j0.46 pu. Control of the load voltage was achieved by regulating the SVC susceptance. The SVC must hold the load voltage around the reference voltage. As a consequence, the SVC susceptance must vary according to the network reactive power needed. Furthermore, the power supplied/absorbed by the SVC varies according to the SVC susceptance. When the load voltage was at a high level due to light loading, the SVC absorbed the reactive power from the network. When the load voltage was at a low level, the SVC supplied reactive power to the network.

The performances of the power systems were improved by increasing of loading margin (λ_1). Computation of the λ_1 was done by using Eq. (12), the results are summarized in Table 6. Table 6 shows that the λ_1 for $V_{ref} = 0.98$ pu was obtained at the value of j0.2 pu. When the V_{ref} was increased to 0.985 pu, the λ_1 expanded to j0.28 pu. Initial reactive load (λ_0) was taken at the value of

j11.27 pu for V_{ref} = 0.98 and 0.985 pu. Next, the V_{ref} was increased at the values of 0.99 and 0.995 pu. And the λ_0 was taken at the value of j11.37 pu. The λ_1 for the V_{ref}=0.99 pu was obtained at the value of j0.37 pu. Finally, the maximum λ_1 for V_{ref} of 0.995 pu was obtained at the value of j0.46 pu. As a consequence, the proposed method was able to expand the saddle-node bifurcation by shifting the loading margin to the right in parameter space.

Based on the simulation results, it can be stated that the proposed method was able to control both chaos and voltage collapse caused by DE and critical reactive loads in power systems. Furthermore, the proposed method was able to control the load voltage to values near the set value.

6. Conclusion

Chaotic oscillation, voltage collapse and their control were closely investigated in this study. Both chaos and voltage collapse exist in power systems due to heavy loading conditions and disturbing of energy. The results presented here show that the proposed method can successfully control and suppress both chaos and voltage collapse. Furthermore, the load voltage can be controlled by adjusting the reactive power supplied by the SVC device. When the reactive load was increased, the SVC susceptance and the reactive power supplied by the SVC also increased in order to maintain reactive power balanced in the system. The load voltage was also improved by the proposed method. Finally, the loading margin was expanded by the proposed method and the maximum loading margin was achieved at the value of j0.46 pu.

References

[1] Chiang H-D, Dobson I, Thomas RJ, Thorp JS, Ahmed LF. On voltage collapse in electric power systems. IEEE Trans Power Syst 1990;5(2).

[2] Mello LF, de Sauza ACZ, Yoshinory GHJr, Schneider CV. Voltage collapse in power systems: dynamical studies from a static formulation. Mathematical problem in engineering. Hindawi Publishing Corp.; 2006.

[3] Chiang H-D, Varaiya PP, Wu FF, Lauby MG. Chaos in a simple power system. IEEE Trans Power Syst 1993;8(4).

[4] Wang HO. Control of bifurcation and routes to chaos in dynamical system. Thesis report Ph.D. USA: Institute for Systems Research, The University of Maryland; 1993.

[5] Wang HO, Abed EH, Hamdan AMA. Bifurcations, chaos, and crises in voltage collapse of a model power system. IEEE Trans Circ Syst 1: Fundam Theory Appl 1994;41(3).

[6] Chiang H-D. Application of bifurcation analysis to power systems. In: Chen G, Hill DJ, Yu X, editors. Bifurcation control: theory and applications. Germany: Springer-Verlag; 2003.

[7] Dobson I. Distance to bifurcation in multidimensional parameter space: margin sensitivity and closest bifurcation. In: Chen G, Hill DJ, Yu X, editors. Bifurcation control: theory and applications. Germany: Springer-Verlag; 2003.

[8] Yu Y, Jia H, Li P, Su J. Power system instability and chaos. In: Proc. of the 14th PSCC, Sevilla; 2002.

[9] Ginarsa IM, Soeprijanto A, Purnomo MH, Implementation of classical model to chaotic identification in power systems due to disturbing of energy. In: Proc. of the 9th seminar on intellegent tech. and app. (SITIA 2008), Surabaya; 2008.

[10] Ginarsa IM, Soeprijanto A, Purnomo MH. Modelling of chaotic behavior in power systems using recurrent neural networks. In: Proc. of the int. conf. intellegent tech. on and app. (ICACIA 2008), Jakarta; 2008.

[11] Parker TS, Chua LO. Chaos: a tutorial for engineers, invited paper. Proc IEEE 1987;75(8).

[12] Chen G. Chaos: control and anti-control. IEEE Circ Syst Soc Newslett 1998;9(1).

[13] Lei Z-M, Liu Z-J, Sun H-X, Liu H-X. Control and application of chaos in electrical system. In: Proc. of the fourth int. conf. on machine learning and cybernatics, Guangzhou; 2005.

[14] Konishi K, Kokame H. Stabilizing and tracking chaotic orbits using a neural network. In: Proceedings of the int. symposium on nonlinear theory and its app. (NOLTA95), Las Vegas, USA; 1995.

[15] Precup RE, Marius ML, Preitl S. Lorenz stabilization using fuzzy controller. Int J Comput Commun Contr 2007;II(3).

[16] Calvo O, Cartwright JHE. Fuzzy control of chaos. Int J Bifurc Chaos 1998;8:1743–7.

[17] Dhamala M, Lai Y-C, Kostelich EJ. Analyses of transient chaotic time-series. Phys Rev E 2001;64.

[18] Dhamala M, Lai Y-C. Controlling transient chaos in deterministic flows with applications to electric power systems and ecology. Phys Rev E 1999;59(2).

[19] Krishnaiah J, Kumar CS, Faruqi MA. Modeling and control of chaotic processes through their bifurcation diagrams generated with the help of recurrent neural network models: part 1 – simulation studies. J Process Contr 2006:53–66.

[20] Zhang J, Wen JY, Cheng SJ, Ma J. A novel SVC allocation method for power system voltage stability enhancement by normal forms of diffeomorphism. IEEE Trans Power Syst 2007;22(4).

[21] Minguez R, Milano F, Minano RZ, Conejo AJ. Optimal network placement of SVC devices. IEEE Trans Power Syst 2007;22(4).

[22] Singh JG, Singh SN, Srivastava SC. An approach for optimal placement of static VAr compensators based on reactive power spot price. IEEE Trans Power Syst 2007;22(4).

[23] Farsangi MM, Pour HH, Song Y-H, Lee KY. Placement of SVCs and selection of stabilizing signals in power systems. IEEE Trans Power Syst 2007;22(3).

[24] Zhijun E, Fang DZ, Chan KW, Yuan SQ. Hybrid simulation of power systems with SVC dynamic phasor model. Int J Elect Power Energy Syst 2009;31:175–80.

[25] Soeprijanto A, Yorino N, Sasaki H. Design of robust coordinated SVC supplementary controllers. Electr Power Syst Res 2001;58:141–8.

[26] Subramanian DP, Devi RPK, Saravanaselvan R. A new algorithm for analysis of SVC's supplementary control to eliminate time delay by wide area signal input. Int J Elect Power Energy Syst 2011;33(5):1194–202.

[27] Yuan Y, Li G, Cheng L, Sun Y, Zhang J, Wang P, et al. A phase compensator for analysis of SVC impact on bifurcation, chaos and voltage collapse in power systems. Int J Elect Power Energy Syst 2010;32:163–9.

[28] Ballal MS, Khan ZJ, Suryawanshi HM, Sonolikar RL. Adaptive neuro-fuzzy inference system for the detection of inter-turn insulation and bearing wear faults in induction motor. IEEE Trans Indus Electron 2008;54(1):250–8.

[29] Sobha M, Kumar RS, George S. ANFIS based supplementary controller for damping low frequency oscillations in power systems, JES on-line; 2007. <http://journal.esrgroups.org/jes/>.

[30] Mitra P, Malik S, Chowdhury SP, Chowdhury SP. ANFIS based automatic voltage regulator with hybrid learning algorithm. Int J Innovat Energy Syst Power 2008.

[31] Kundur P. Power system stability and control, EPRI. New York: McGraw-Hill; 1994.

[32] Alligood KT, Sauer TD, Yorke JM. Chaos: an introduction to dynamical systems. New York: Springer-Verlag; 2000.

[33] Zhang X-P, Rehtanz C, Pal B. Flexible AC transmission systems: modelling and control. Berlin: Springer-Verlag; 2006.

[34] Jang J-SR, Sun CT, Mizutani E. Neuro-fuzzy and soft computing: a computational approach to learning and machine intelligence. USA: Prentice-Hall International, Inc.; 1997.

[35] Jang J-SR, Sun CT, Mizutani E. MATLAB version 7.6 (2008a): the language of technical computing. The Matworks Inc.; 2008.